High-Resolution Studies of (d,p) Reactions on Cd^{114} and In^{115}†

J. B. MOORHEAD, B. L. COHEN, AND R. A. MOYER
University of Pittsburgh, Pittsburgh, Pennsylvania
(Received 5 September 1967)

Energy and angular distributions from 12-MeV deuteron-induced (d,p) reactions on Cd^{114} and In^{115} were measured with ~8-keV energy resolution. In $In^{115}(d,p)$ essentially all components of the $(\pi g_{9/2}^{-1})$ $(\nu h_{11/2})$ configuration are located, and I values are estimated from sum rules. I values for many members of the $(\pi g_{9/2}^{-1})$ $(\nu d_{3/2})$ and $(\pi g_{9/2}^{-1})$ $(\nu s_{1/2})$ are determined from sum rules and the presence or absence of $l=0$ and $l=2$ mixing. As in a previous study of $Pd(d,p)$, there is a large excess of $g_{7/2}$ and a large deficiency of $h_{11/2}$ strength relative to the isotonic tin nucleus (Sn^{116}) and expectations from nuclear-structure theory. The most obvious experimental explanations for this discrepancy are discussed and found not to be applicable.

I. INTRODUCTION

THIS is the second paper in a new series of high-energy-resolution investigations with stripping reactions of nuclear structure in nonclosed-shell nuclei in the $N=50$ to 82 shell. In the first paper of this series[1] studies of two odd-A palladium isotopes were reported; in this paper we report on a third odd-A nucleus, Cd^{115}, and on an odd-odd nucleus, In^{116}. Both of these are isotonic with Sn^{117}, whose structure is among the best understood in this mass region,[2] so intercomparisons among the three, as well as comparisons with the Pd isotopes, are most enlightening.

Experimental studies of (d,p) reactions on Cd^{114} have been reported by Rosner[3] and by Silva and Gordon,[4] and a similar study on In^{115} has been reported by Hjorth and Allen.[5] In all of this work, the resolution was nearly an order of magnitude worse than in the present experiments, so only the most strongly excited peaks could be identified. However, the work by Rosner[3] included measurements on $Cd^{116}(d,t)$ reactions exciting the states of Cd^{115}, which were useful in our analysis.

II. EXPERIMENTAL

The measurements were carried out with 12-MeV deuterons from the University of Pittsburgh Tandem Van de Graaff accelerator bombarding thin targets of Cd^{114} and In^{115}. Protons from (d,p) reactions were magnetically analyzed with an Enge split-pole spectrograph and detected by photographic plates. The essentials of the experimental method and the various factors affecting the energy resolution were discussed in considerable detail in Ref. 1; only variations from them will be described here. Measurements were made at about 12 angles between 8° and 55°; typical proton energy spectra are shown in Figs. 1 and 2. The product of the integrated incident beam and the target thickness

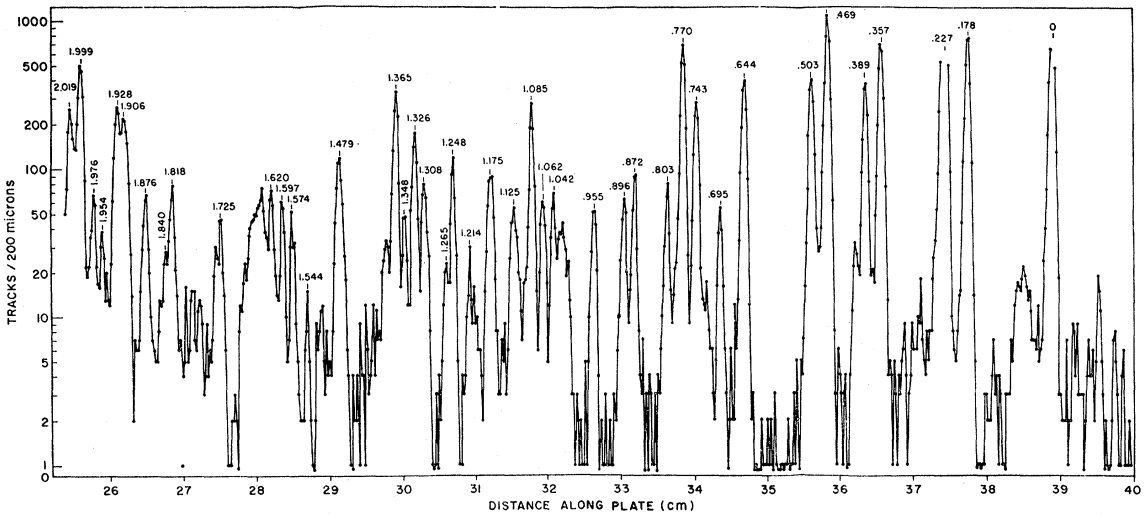

FIG. 1. Typical energy spectrum. This is the energy spectrum of protons from $Cd^{114}(d,p)$ with protons detected at 50°. Numbers above peaks are excitation energies of corresponding levels in the residual nucleus Cd^{115} in MeV. Unlabeled peaks are due to impurities.

† Supported by National Science Foundation.
[1] B. L. Cohen, J. B. Moorhead, and R. A. Moyer, Phys. Rev. **161**, 1257 (1967).
[2] E. J. Schneid, A. Prakash, and B. L. Cohen, Phys. Rev. **156**, 1316 (1967).
[3] B. Rosner, Phys. Rev. **136**, B664 (1964).
[4] R. J. Silva and G. E. Gordan, Phys. Rev. **136**, B618 (1964).
[5] S. A. Hjorth and L. H. Allen, Arkiv Fysik **33**, 121 (1966).

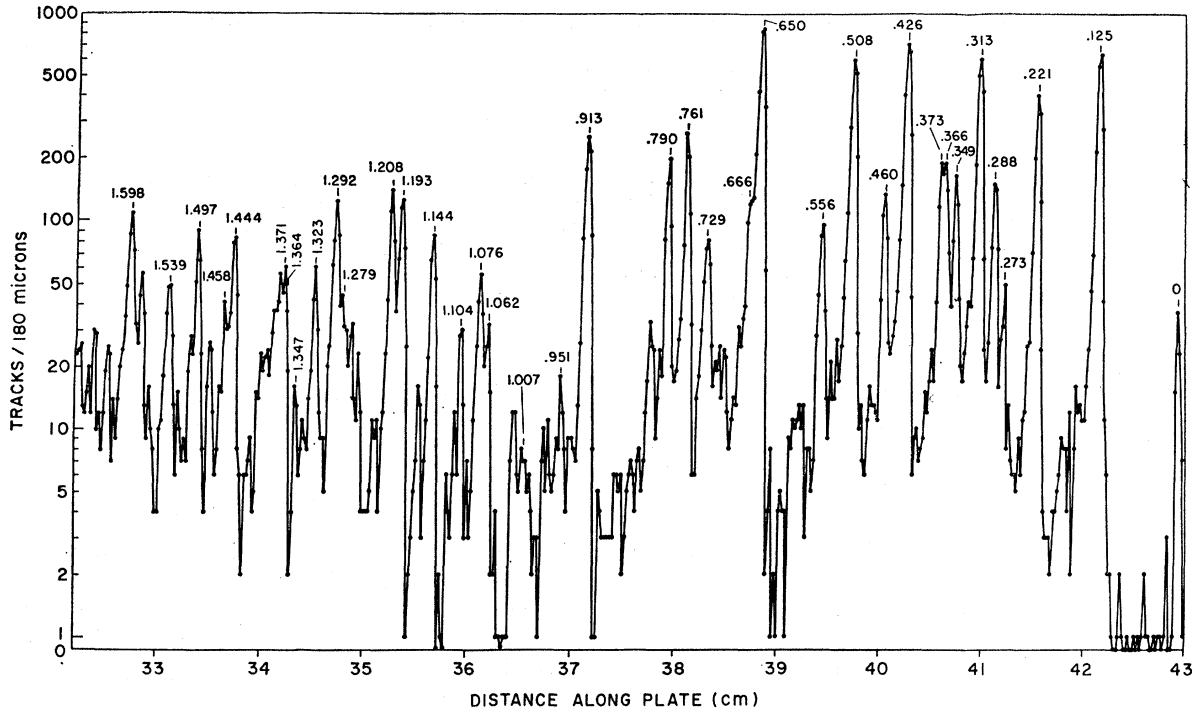

FIG. 2 Energy spectrum of protons from $In^{115}(d,p)$. See caption to Fig. 1.

was determined by observing elastically scattered deuterons at $\pm 40°$ with surface-barrier detector monitors. The pulse-height spectrum from each was recorded on separate multichannel analyzers; dead-time corrections were obtained by feeding every one-hundredth elastic proton pulse from one detector simultaneously into a scaler and the "external clock" input of the analyzer recording the spectrum from the other detector. Typical dead times were 5–10%. The energy resolution in the monitor spectra was easily good enough to separate out the elastic peak from other peaks (due to carbon and oxygen). The elastic-scattering cross sections for Cd and In were taken from Ref. 6. The use of two monitors at equal angles on opposite sides of the beam cancels the largest errors due to uncertainty in the angle and position at which the beam strikes the target. In the work reported here, the accuracy in positioning the monitors left something to be desired—this has since been corrected—and this gives perhaps the largest over-all uncertainty to the cross-section measurements. In general, the cross sections should be accurate to about $\pm 10\%$ for cleanly resolved peaks containing several hundred tracks. The principal difficulty in the accuracy of cross-section determinations arises from contributions to the spectrum from impurities where these are not cleanly resolved as separate peaks.

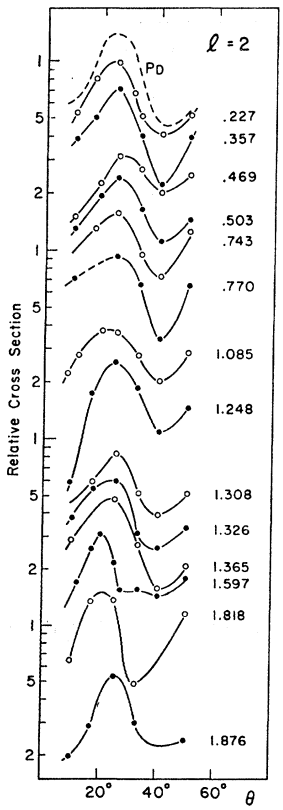

FIG. 3. Angular distributions of protons from $Cd^{114}(d,p)Cd^{115}$ corresponding to $l=2$ transitions. Dashed curve above is a typical $l=2$ angular distribution for Pd from Ref. 1. Numbers on right are excitation energies of corresponding levels in the residual nucleus Cd^{115} in MeV.

Both the Cd^{114} and In^{115} targets were more than 99% isotopically pure, so isotopic impurities were of little consequence. Target thicknesses were typically about 50 $\mu g/cm^2$.

[6] G. Mairle and U. Schmidt-Rohr, Max Planck Institut für Kernphysik (Heidelberg) Report No. 19651 V113 (unpublished).

In some parts of this work the target slit was somewhat wider than that used in Ref. 1—1.0 mm versus 0.4 mm. This allows the beam to be tuned completely off the target slit, which almost completely eliminates background. Although this worsens the energy resolution—typically from 7.0 to 8.5 keV—it is often well worth that price. In more recent work this problem has been eliminated by evaporating the target material on the carbon backing as a very thin strip, so the target slit can be made very wide without affecting the energy resolution.

III. RESULTS AND ANALYSIS—$Cd^{114}(d,p)$

The angular distributions of the various proton groups from the $Cd^{114}(d,p)$ reaction are shown in Figs. 3–7. Results from an earlier set of runs were much less consistent due to monitoring difficulties, so they are generally not shown here, although they were very useful in peak identification and are used in the angular distributions where the newer data are obscured by impurity peaks. In Figs. 3–7 the angular distributions are grouped according to their l-value assignments, which were obtained from comparisons with distorted-wave Born-approximation (DWBA) calculations, previous experience,[1] and angular distributions of levels with known angular momentum and parity.

The results of DWBA calculations, carried out with code JULIE,[7] are shown in Fig. 8 for Pd^{108} and Sn^{116} with $Q=4.0$ MeV. The Perey "average" parameters[8] recommended by Winner and Drisko[9] were used. In general, the shifts between the two targets in both angle and magnitude are small enough to allow simple interpolation for the target nuclei studied here. Moreover, the experience with other DWBA calculations for Pd^{108}, reported in Ref. 1, can still be considered valid, so that no further calculations were made. Typical experimental angular distributions from Pd are shown as dashed curves in Figs. 3, 4, and 5. There seems to be somewhat less variation with target mass than is suggested by

[7] Code JULIE of R. Bassel, R. M. Drisko, and G. R. Satchler (unpublished). Optical-model parameters used were

		Pd^{108}	Sn^{116}
Deuterons:	r'	1.15	1.15
	r_0'	1.34	1.34
	r_c	1.15	1.15
	a	0.81	0.81
	a'	0.68	0.68
	V	98	99
	W'	17.2	17.2
	V_{SO}	...	...
Protons:	r'	1.25	1.25
	r_0'	1.25	1.25
	r_c	1.25	1.25
	a	0.65	0.65
	a'	0.47	0.47
	V	53.7	53
	W'	13.5	13.5
	V_{SO}	7.8	7.5

[8] F. G. Perey, Phys. Rev. 131, 745 (1963).
[9] D. R. Winner and R. M. Drisko, University of Pittsburgh Technical Report, 1965 (unpublished).

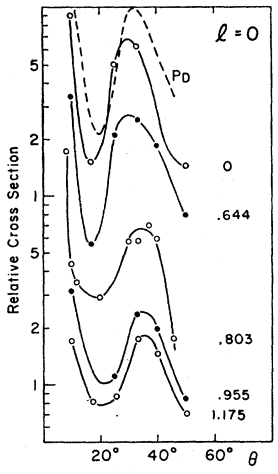

FIG. 4. Angular distributions of protons from $Cd^{114}(d,p)Cd^{115}$ corresponding to $l=0$ transitions. See caption to Fig. 3.

Fig. 8. The experimental angular distribution for the $l=2$ transitions are much more sharply peaked than those calculated with the DWBA. This is true for Pd as well as Cd.

The energies of the levels, the l-value assignments, and the comparison with previous data are given in Table I. In general, the agreement with previous results is quite satisfactory. Also listed in Table I are cross sections at the peak of the angular distributions, $I\pi$ assignments, and spectroscopic factors. The assignments for $l=0$, 4, and 5 were made from shell theory as $1/2^+$, $7/2^+$, and $11/2^-$, respectively. For the $l=2$ states one expects[2] the low-lying states to be mostly $3/2^+$ and the higher-lying states to be $5/2^+$. The assignments for the weakly excited states were made in this manner, but the four most strongly excited states were assigned by Rosner[3] on the basis of the ratio of (d,p) to (d,t) cross sections for exciting the same states; these assignments are used in Table I. The spectroscopic factors were obtained from the well-known relationship

$$d\sigma/d\Omega = 1.5(2j+1)S\sigma_{DW} \quad \text{(even-even)}, \qquad (1)$$

where σ_{DW} is the cross section from the DWBA calculation. Following the usual procedure, S was calculated from (1) at the peak of the angular distribution.

The spectroscopic factors from Table I are plotted versus excitation energy for the various single-particle

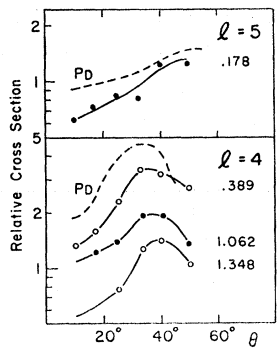

FIG. 5. Angular distributions of protons from $Cd^{114}(d,p)Cd^{115}$ corresponding to $l=4$ and $l=5$ transitions. See caption to Fig. 3.

TABLE I. Energy levels and spin assignments for Cd^{115} and cross sections for the (d,p) reactions leading to them.

Present work					Rosner[a]			Silva and Gordon[b]	
(1) Excitation energy (MeV)	(2) $\sigma(d,p)$[c] (mb/sr)	(3) l	(4) s	(5) J^π	(6) Excitation energy (MeV)	(7) l	(8) J^π	(9) Excitation energy (MeV)	(10) J^π
g.s.	2.80	0	0.35	$1/2^+$	g.s.	0	$1/2^+$	0	$1/2^+$
0.178	0.46	5	0.33	$11/2^-$	0.18	5	$11/2^-$	0.173	$11/2^-$
0.227	2.29	2	0.53	$3/2^+$	0.23	2	$3/2^+$	0.224	$3/2^+,5/2^+$
0.357	0.72	2	0.096	$5/2^+$	0.36	2	$5/2^+$	0.362	$3/2^+,5/2^+$
0.389	0.27	4	0.27	$7/2^+$					
0.469	0.82	2	0.184	$3/2^+$	0.48	(4,2)	$(7/2^+,3/2^+)$	0.467	$3/2^+,5/2^+$
0.503	0.45	2	0.103	$3/2^+$					
0.644	0.70	0	0.085	$1/2^+$	0.65	0	$1/2^+$	0.639	$1/2^+$
0.695	0.03	(3)	0.0023	$(7/2^-)$					
0.743	0.21	2	0.049	$3/2^+$					
0.770	0.55	2	0.126	$3/2^+$	0.77	2	$3/2^+$	0.765	$3/2^+,5/2^+$
0.803	0.05	0	0.0061	$1/2^+$					
0.872	0.05	3	0.0040	$7/2^-$					
0.896	0.04				0.89	(4)	$(7/2^+)$		
0.955	0.12	0	0.014	$1/2^+$	0.96	0	$1/2^+$		
1.042	0.04	(1)	0.0018	$(3/2^-)$					
1.062	0.04	4	0.045	$7/2^+$					
1.085	0.19	2	0.024	$5/2^+$	1.10	2	$5/2^+$	1.084	$3/2^+,5/2^+$
1.125	0.04								
1.175	0.17	0	0.021	$1/2^+$	1.19	0	$1/2^+$	1.163	
1.214	0.03	3	0.024	$7/2^-$					
1.248	0.10	2	0.012	$(5/2^+)$					
1.265					1.26	2	$3/2^+$		
1.308	0.08	2	0.011	$(5/2^+)$				1.309	
1.326	0.17	2	0.022	$(5/2^+)$					
1.348	0.03	(4)	0.029	$(7/2^+)$					
1.365	0.36	2	0.047	$(5/2^+)$	1.37	2	$(5/2^+)$	1.359	$3/2^+,5/2^+$
1.479									
1.544									
1.574									
1.597	0.04	2	0.005	$(5/2^+)$					
1.620	0.08	(2,0)	0.0092, 0.0030	$(5/2^+,1/2^+)$					
1.725									
1.818	0.06	2	0.0071	$(5/2^+)$					
1.840	0.06	(2,0)	0.0040, 0.0047	$(5/2^+,1/2^+)$					
1.876	0.10	(2)	0.013	$(5/2^+)$					
1.906	0.25	(2,4)	0.021, 0.125	$(5/2^+,7/2^+)$					
1.928	0.39	(1)	0.016	$(3/2^-)$				1.927	$(3/2^+,5/2^+)$
1.954									
1.976	0.08	(2,4)	0.079, 0.026	$(5/2^+,7/2^+)$					
1.999	0.76	1	0.032	$3/2^-$					
2.019	0.32	1	0.013	$3/2^-$				2.015	$(1/2^-,3/2^-)$

[a] See Ref. 3. [b] See Ref. 4. [c] Measured at first peak beyond 10°.

states in Fig. 9. Also shown in Fig. 9 are the energies E_j of the "center of gravity" of all levels belonging to each single-particle state (obtained by weighting each state according to its S value), the corresponding quantity from $Sn^{116}(d,p)$ reactions, and the sum of the spectroscopic factors $\sum S$, for each single-particle state. The former quantities are listed in Table II. The latter quantity is interpreted as the "emptiness" U_j^2 of the

TABLE II. E_j for various single-particle states.

	Cd^{114}	In^{115} (−0.25)	Sn^{116}
$s_{1/2}$	0.23	0	0
$d_{3/2}$	0.42	0.25	0.16
$h_{11/2}$	0.18	0.22	0.32
$g_{7/2}$	0.95	···	0.72
$d_{5/2}$	1.15	···	1.30

TABLE III. Sum of spectroscopic factors $\sum S$; or "emptiness" U_j^2 for various single-particle states.

S.P. state \ Target	Cd^{114}	In^{115}	Sn^{116}	Sn^{116} (15 MeV)[a]	Sn^{116} Renorm[a]
$s_{1/2}$	0.55	0.48	0.62	0.65	0.49
$d_{3/2}$	1.00	0.75	0.84	0.55	0.64
$h_{11/2}$	0.33	0.62	0.69	0.81	0.85
$g_{7/2}$	0.52	0.67	0.18	0.13	0.13
$d_{5/2}$	0.28	0.10	0.19	0.14	0.18

[a] See Ref. 2.

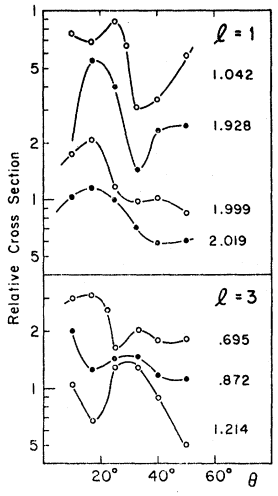

FIG. 6. Angular distributions of protons from $Cd^{114}(d,p)Cd^{115}$ corresponding to $l=1$ and $l=3$ transitions. See caption to Fig. 3.

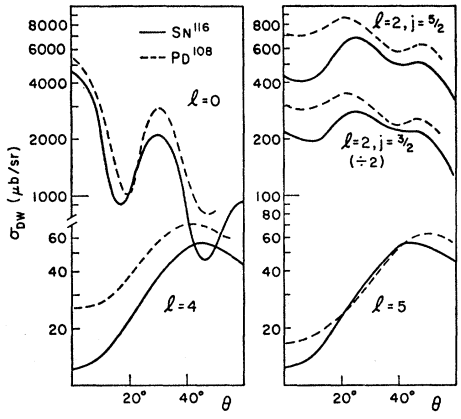

FIG. 8. Theoretical angular distributions from DWBA calculations using the code JULIE. See Ref. 7. Solid curves are for $Sn^{116}(d,p)Sn^{117}$, dashed curves for $Pd^{108}(d,p)Pd^{109}$. Curves were obtained using proton and deuteron optical-model parameters from Ref. 8.

single-particle state j. The $\sum S$ are listed and compared with the corresponding quantities from other targets in Table III.

IV. RESULTS AND ANALYSIS: $In^{115}(d,p)$

The angular distributions from the $In^{115}(d,p)In^{116}$ reactions are shown in Figs. 10–13. Although mixing of l values is expected in targets of nonzero spin [In^{115} is $9/2^+$, arising from a $(g_{9/2})^{-1}$ proton configuration], all angular distributions are fairly well characterized by one principal l value, and they are grouped in this way in the figures. Actually, they were fitted to a sum of all possible l values, and where the accuracy of the data warranted, cross sections for each l value were obtained. It is clear from Fig. 10, for example, that the high cross sections at forward angles and near 33° for the 0.313-MeV level require an $l=0$ mixture; it is likewise apparent from Fig. 11 that the 0.221- and 0.426-MeV levels have extra intensity between 20–25° as compared with the 0.125-MeV peak and the $l=0$ peaks from $Cd^{114}(d,p)$ in Fig. 4, so they very probably contain admixtures of $l=2$. The same might be said of the 0.273-MeV state, but it is so weakly excited that statistical errors make conclusions questionable, and it is not important enough in the analysis to concern us greatly.

The most impressive feature of these data is that there are as many $l=5$ states as expected theoretically.

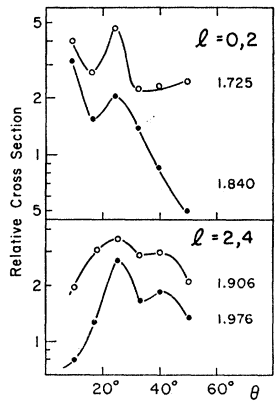

FIG. 7. Angular distributions of protons from $Cd^{114}(d,p)Cd^{115}$ corresponding to mixtures of $l=0$ and $l=2$ and to mixtures of $l=2$ and $l=4$. See caption to Fig. 3.

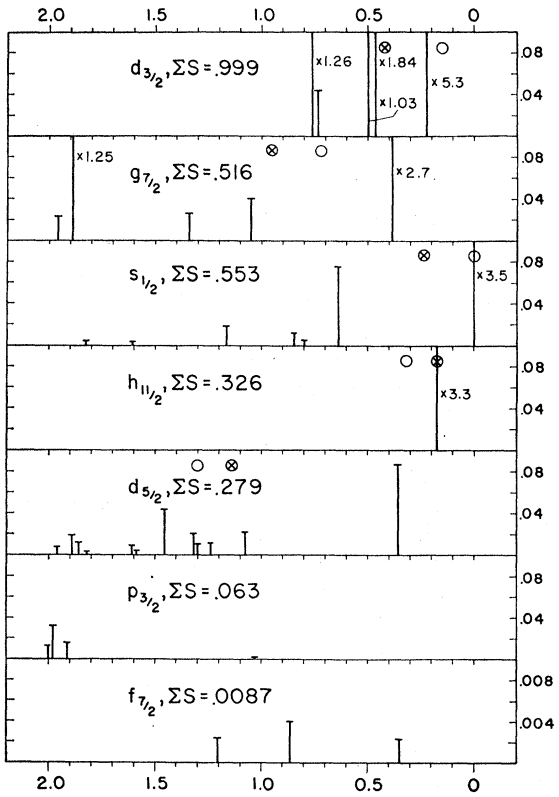

FIG. 9. Spectroscopic factors versus excitation energy for various single-particle states of Cd^{115}. The height of the vertical lines is proportional to the spectroscopic factors of the respective states. Multipliers appear to the right of states for factors larger than full scale. Circumscribed X's show centers of gravity of all levels belonging to each single-particle state. Empty circles are centers of gravity for $Sn^{116}(d,p)$.

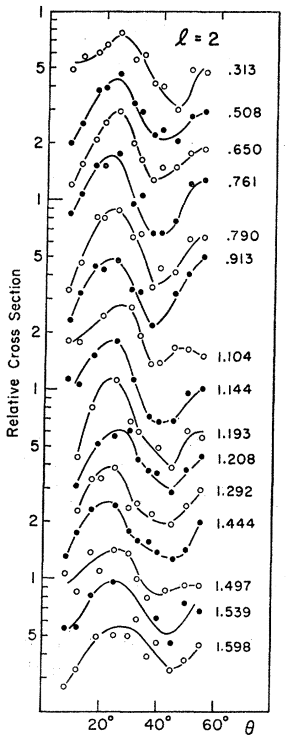

FIG. 10. Angular distributions for protons from $In^{115}(d,p)In^{116}$ corresponding to $l=2$ transitions. Numbers on right are excitation energies of corresponding levels in the residual nucleus In^{116} in MeV.

These are clearly distinguished from low-l states by the large angle of the first peak in their angular distribution, and from $l=4$ states by the fact that the latter drop much more steeply in the forward direction as predicted by DWBA calculations and verified by the 0.0-MeV state whose known $I\pi$ of 1^+ requires $l=4$. The 0.266- and 0.373-MeV states could not be resolved at small angles, but their ratio at large angles—shown in Fig. 12—is so constant that it is fair to presume that their angular distributions are the same. The 0.666- and 0.729-MeV states have atypical angular distributions, but no other l-value assignment seems more likely experimentally, or is as easily explained theoretically. The $l=1$ assignments in Fig. 12 seem reasonably certain, but the $l=3$ assignments there are rather questionable. As they play no part in the analysis, we will ignore this problem.

The results for the $In^{115}(d,p)$ reaction are summarized in Table IV. The basic formula for extracting spectroscopic information from odd target nuclei is

$$\frac{d\sigma}{d\Omega}=1.5\times\frac{2I+1}{2I_t+1}S\sigma_{DW}\quad\text{(odd-}A\text{)},\qquad(2)$$

where I_t and I are the angular momenta of the target and final nuclei. Since I is not usually known, the most useful quantity here[10] is S', defined as

$$S'=\frac{d\sigma/d\Omega}{1.5\sigma_{DW}}=\frac{2I+1}{2I_t+1}S,\qquad(3)$$

where the first expression, the definition, is used in obtaining S' from experimental data for $d\sigma/d\Omega$, and the last is derived from it by use of (2). The values of S' from the $In^{115}(d,p)$ reaction are listed in Table IV. In the few cases where there was some correspondence between the energies and l values of Ref. 5, the agreement in S' values is reasonably good. In general, however, the work of Ref. 5 is severely limited by the fact that the average level spacing in Table IV is about 30 keV, whereas the energy resolution in Ref. 5 was about 60 keV. The energy of the first excited state in Ref. 5 is 150 keV as compared to 125 keV here. The higher levels, where recognizable, are similarly displaced. We can offer no simple explanation for this discrepancy, since energy resolution is not a factor in it. In Ref. 11, the energy of the first excited state, derived rather indirectly, is listed as 70 keV.

The values of S' are plotted versus energy of the levels for the various l assignments in Fig. 14. Also shown in

TABLE IV. Results for $In^{115}(d,p)In^{116}$.

Excitation energy (MeV)	l	σ_{max} (μb/sr)	S'	I^π	S'[a]
0	4	14.5	0.20	1^+	0.14
0.125	0	1350	0.45	5^+	0.32
0.221	0	620	0.20	4^+	0.17
	2	90	0.12		
0.273	0	23	0.008	$4^+,5^+$	
0.288	5	85	1.07	8^-	
0.313	2	440	0.56	5^+	
	0	100	0.033		
0.349	5	72	0.90	$5^-,6^-,7^-,9^-$	
0.366	5	70	0.87	$5^-,6^-,7^-,9^-$	
0.373	5	90	1.13	$9^-,10^-$	
0.426	0	700	0.23	4^+	
	2	340	0.43		
0.460	5	75	0.92	$5^-,6^-,7^-,9^-$	
0.508	2	480	0.57	3^+	0.25
0.556	5	52	0.62	$3^-,4^-,5^-$	
0.650	2	720	0.86	6^+	0.42
0.666	5	75	0.87	$5^-,6^-,7^-,9^-$	
0.729	5	50	0.57	$3^-,4^-,5^-$	
0.761	2(1)	160	0.18	2^+-7^+	
0.790	2	125	0.14	2^+-7^+	
0.913	2	150	0.16	2^+-7^+	
0.951	1(?)	33	0.007	3^--6^-	
1.007	1(?)	10	0.002	3^--6^-	
1.062	3	19	0.027	2^--7^-	
1.076	?	40	...	...	
1.104	2(?)	40	0.034	2^+-7^+	
1.144	2	76	0.065	2^+-7^+	
1.193	2	120	0.102	2^+-7^+	
1.208	2	120	0.102	2^+-7^+	
1.279	4	35	0.36	8^+	
1.292	2	105	0.085	2^+-7^+	
1.323	5	28	0.30	$(2)^-$	
1.347	(5)	~10	0.10	(1^-)	
1.364	0	27	0.008	4^+-5^+	
1.371	(+2?)	65	0.019	4^+-5^+	
1.444	2	80	0.065	2^+-7^+	
1.458	3	24	0.032	2^--7^-	
1.497	2(3)	64	0.049	2^+-7^+	
1.539	2	46	0.035	2^+-7^+	
1.598	2	100	0.077	2^+-7^+	

[a] See Ref. 5.

[10] B. L. Cohen and O. V. Chubinsky, Phys. Rev. **131**, 2184 (1963).

[11] *Nuclear Data Sheets*, compiled by K. Way *et al.* (Printing and Publishing Office, National Academy of Sciences—National Research Council, Washington 25, D. C., 1960).

Fig. 14 are $\sum S'$ and the sum rule predictions of $\sum S'$ for each I. These are derived as follows:

Let us assume that the fullness of a given single-particle state in an even-even nucleus is the same as in an isotonic odd nucleus. The summed cross sections in the two cases are therefore the same, or

$$\sum \frac{d\sigma}{d\Omega}\Big|_e = \sum \frac{d\sigma}{d\Omega}\Big|_0, \tag{4}$$

where the sums are over-all components of a given single-particle state j. From (1), (2), and (3), Eq. (4) gives

$$\sum S_0' = (2j+1)\sum S_e. \tag{5}$$

The strength of excitation of the various I components in the case of the odd target is proportional to $2I+1$, so the strength for a given I is

$$(2I+1)/\sum_{I'=|I_t-j|}^{I_t+j}(2I'+1)$$

of the total. The sum in the denominator is

$$\sum_A^B (2I+1)=\sum_0^B (2I+1)=\sum_0^{A-1}(2I+1)=(B+1)^2-(A)^2$$
$$=(I_t+j+1)^2-(I_t-j)^2=(2I_t+1)(2j+1).$$

Thus the sum of S' for transitions leading to final states of angular momentum I, $\sum S_I'$ is

$$\sum S_I' = \frac{2I+1}{2I_t+1}\sum S_e. \tag{6}$$

$\sum S_e$ may be expressed in terms of the emptiness U_j^2 of the single-particle state j as $\sum S = U_j^2$, whence (5) and (6) become, respectively,

$$\sum S' = (2j+1)U_j^2 \tag{5'}$$

and

$$\sum S_I' = \frac{2I+1}{2I_t+1}U_j^2. \tag{6'}$$

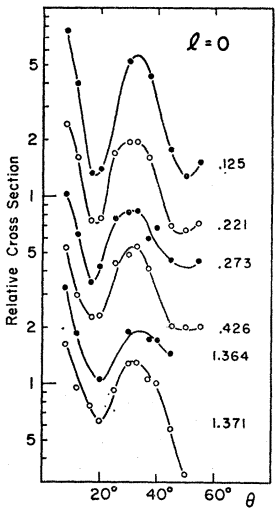

FIG. 11. Angular distributions for protons from $In^{115}(d,p)In^{116}$ corresponding to $l=0$ transitions. See caption to Fig. 10.

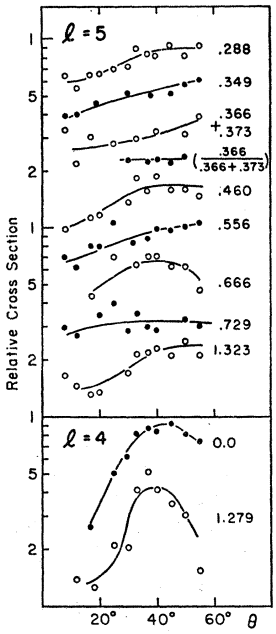

FIG. 12. Angular distributions for protons from $In^{115}(d,p)In^{116}$ corresponding to $l=5$ and $l=4$ transitions. See caption to Fig. 10.

By use of (5'), U_j^2 may be determined directly from the data. The values are given in Fig. 14 and are listed in Table III, where they are compared with the values for Cd^{114} and Sn^{116}. An entirely different procedure was used for the $g_{7/2}$ state; it will be discussed below. In applying the above procedure to the $l=2$ states, some decision must be made as to whether a state is $d_{5/2}$, $d_{3/2}$, or some particular mixture of the two. In general, one expects the low-lying states to be $d_{3/2}$ and the higher states to be $d_{5/2}$. From the data for Sn^{116} and Cd^{114} in Table III, one expects the ratio $U_{3/2}^2/U_{5/2}^2$ to be about 3.5. This ratio is roughly obtained if all $l=2$ levels below 0.9 MeV are assumed to be $d_{3/2}$ and those above that energy to be $d_{5/2}$. This assumption was therefore used. It is surely not completely correct, but it also seems probable that it cannot lead to large errors.

Once the U_j^2 is determined, the $\sum S_I'$ for each I may be determined from (6'). The results are shown in Fig. 14 by the horizontal hashmarks with I values attached. We now consider the results in an attempt to determine I values for the nuclear states. But first we must give some consideration to the types of mixing one might expect.

The nuclear-structure situation is illustrated in Fig. 15. The low-lying states of In^{116} may be considered to consist of a single hole in the 28–50 proton shell coupled to a neutron single-quasiparticle state. The proton-hole states are shown at the left in Fig. 15; the location of $(p_{1/2})^{-1}$ is well known from isomerism in In isotopes; the $(p_{3/2})^{-1}$ and $(f_{5/2})^{-1}$ are not known, but their location is estimated to be at about 1 MeV. The neutron single-quasiparticle states, well known from Sn^{117}—and confirmed by the above data on Cd^{115}—are shown in the second column. The even- and odd-parity configurations obtained by combining these are shown in the third and fourth columns respectively. The con-

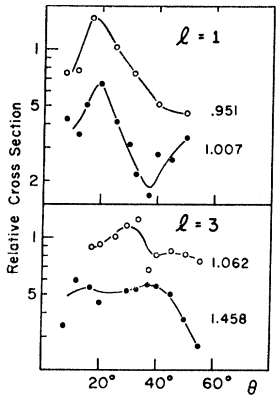

FIG. 13. Angular distributions for protons from $In^{115}(d,p)In^{116}$ corresponding to $l=1$ and $l=3$ transitions. See caption to Fig. 10.

figurations marked by a cross are those which can be excited by (d,p) reactions bombarding the ground state of In^{115}. However, where there are configurations of the same angular momentum and parity nearby, mixing may occur, so that more than one nuclear state for each I is excited.

Now let us consider the situation in Fig. 14 for each neutron single-particle state in turn. According to Fig. 15, the $h_{11/2}$ states—or more correctly, states containing the $(g_{9/2})^{-1}h_{11/2}$ configuration—can have no mixing for $I>6$, and in fact, very little mixing is expected for $I>2$. It would thus be reasonable to expect one state each with $S'=\sum S_I'$ for $I=3$ to 10.

Experimentally, the situation is somewhat clouded by the fact that all of these states are rather weakly excited (see Fig. 2), whence statistical uncertainties are large. Moreover, backgrounds from impurities and other sources have an especially large effect. Thus even the relative values of S' are uncertain by about 20%. Only by use of this large uncertainty can one explain the results. The lowest-energy state is known[11] to be $I=8$; its S' value is in very good agreement with this assignment. The other states are then assigned as shown in Fig. 14, by comparing their S' values with $\sum S_I'$, taking into account experimental uncertainties. The number of levels found is at least correct, and a consistent set of assignments is possible. Actually, one does not expect to see all of these levels, since, by comparing the average level spacing with the experimental energy resolutions, one estimates that about 20% of the weakly excited states (including all the $h_{11/2}$) should be missed. It is also possible that one or two of the $h_{11/2}$ levels shown here have been misassigned, as discussed in connection with the angular distributions.

Among the $s_{1/2}$ states, the experimental accuracy is much better, since the cross sections are large, but the complication from mixing with $l=2$ states sometimes causes difficulties. The 0.125-MeV state has been measured to be $I=5$. If either the 0.221- or 0.426-MeV state was also $I=5$, the $\sum S'$ would be far too large for $I=5$ and far too small for $I=4$; thus both those states must be 4^+. To satisfy the sum rules, most of the other states must be 5^+.

Among the $d_{3/2}$ states, the sensitivity to even very small $l=0$ admixtures is very great, so we may conclude that the 0.650 and 0.508-MeV states, where no such admixtures were found, are very probably $I=6$ and 3 respectively. The former assignment is strengthened by the fact that it is too strongly excited to have a much lower I. The 0.426-MeV state has already been identified as $I=4$. If the 0.313-MeV state, which must be $I=4$ or 5 since it includes an $l=0$ admixture, were also $I=4$, the sum rule for $I=4$ would be greatly exceeded; we therefore conclude that the 0.313-MeV level must be $I=5$.

The situation with the $g_{7/2}$ states is very much complicated by the fact that all its components except $I=1$ and 8 can mix with $l=2$ and/or $l=0$ transitions. Since σ_{DW} is an order of magnitude larger for $l=2$ than for $l=4$, and much larger still for $l=0$, it would be very difficult to detect $l=4$ components. Thus most of them are not seen. On the other hand, it would be very easy to determine even a minute $l=2$ admixture in an $l=4$ angular distribution because of the very low intensity of the latter near 20°. It is clear from Fig. 12 that $l=2$ admixtures in the 0.0- and 1.279-MeV states are almost certainly absent. The former is known to be $I=1$, so that the latter is very probably $I=8$; its intensity would definitely preclude $I=1$ (cf. below). Since $I=1$ is the ground state and there are no other 1^+ configurations that can be reached without crossing major shells (cf. Fig. 15), it seems virtually certain that it is a pure $(g_{9/2})^{-1}g_{7/2}$ state with no mixing. It is therefore used with Eq. (6′) to determine $U_{7/2}{}^2$ for Table III, and that value of $U_{7/2}{}^2$ is used with Eq. (5′) to determine $\sum S'$ in Fig. 14.

As one goes from an even to an odd proton target, a single state in the former couples to the odd proton to give several states. In studying E_j for the two cases, the meaningful comparison would be between the "center" of these several states and the corresponding state in the even proton target. Thus E_j in In^{116} should not be

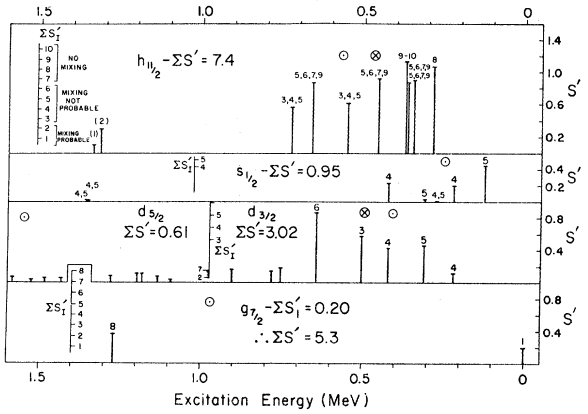

FIG. 14. Spectroscopic factors versus excitation energy for various single-particle states of In^{116}. See caption to Fig. 9. Numbers above peaks are most probable values for I. The scales at the left are the total S_I' expected for each value of I.

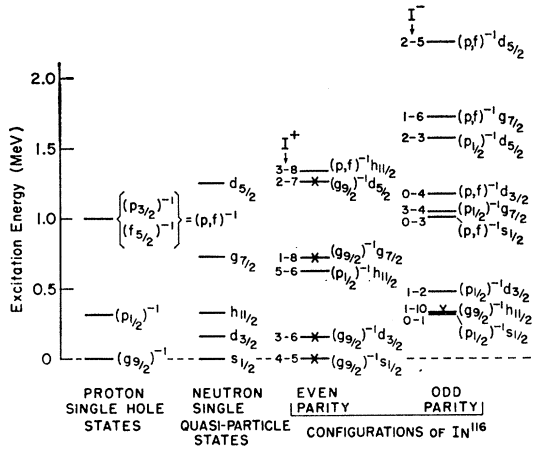

FIG. 15. Configurations of In^{116}. Configurations marked by X's correspond to the ground state of In^{115} plus a neutron in one of the various single-quasiparticle states.

measured from the ground state but from the center of the states into which the ground states of isotonic even proton nuclei are split. This is the center of the $s_{1/2}$ states in Fig. 14. Taking this as the zero, the E_j for the other neutron single-particle states in Sn^{117} are shown by the open circles. Best estimates of E_j from the data for In^{116} are also shown in Fig. 14 and in Table II.

V. DISCUSSION

The principal results of this work are summarized in Tables II and III. The most striking discrepancies there are in the U_j^2 for the $g_{7/2}$ and $h_{11/2}$ states: The $h_{11/2}$ is apparently much more full, and the $g_{7/2}$ is apparently less full in Cd^{114} and In^{115} than in Sn^{116}. Since $g_{7/2}$ is one of the lowest-energy single-particle states in the shell, and $h_{11/2}$ is one of the highest, one expects the former to be nearly full and the latter to be nearly empty, in agreement with the results for tin, but in disagreement with the results for Cd^{114} and In^{115}. A very similar situation was found in the Pd isotopes,[1] where $\sum S$ values indicated that the $h_{11/2}$ state is about 72% full and the $g_{7/2}$ state is only about 20% full. A discussion both of possible experimental and of possible nuclear-structure explanations of this effect was given in Ref. 1, and much of that discussion is also pertinent here. Explanations of the former type are based on a possible error in code JULIE (or invalidity of DWBA) plus the experimental missing of some $h_{11/2}$ peaks; the principal explanation from nuclear-structure theory would require that these nuclei be very nonspherical.

The ease with which $h_{11/2}$ states were located in $In^{115}(d,p)$ would seem to indicate that not many of these states were missed in Pd^{106}, Pd^{108}, and $Cd^{114}(d,p)$ reactions; moreover, no $11/2^-$ configurations with which $h_{11/2}$ could mix are expected below 2 MeV in these nuclei, so that it would be difficult to explain how important components of the $h_{11/2}$ state could arise, let alone be missed in all three even isotopes. On the other hand, the explanation based on uncertainties about the DWBA would seem to be ruled out as a major source of error by the new measurements on $Sn^{116}(d,p)$, which give substantial agreement with the older measurements and with theory.

The DWBA explanation for the large $\sum S$ for $g_{7/2}$ is also greatly weakened by the new measurements for $Sn^{116}(d,p)$, which again give reasonable agreement with the older measurements and with theory. There is perhaps some chance that $g_{7/2}$ states other than the 0.72-MeV state will be found in $Sn^{116}(d,p)$—they are currently being searched for. The only other experimental explanation would be in misassignments of states as $l=4$. In $In^{115}(d,p)$ there is no possibility of this, as the results are based entirely on the transition to the ground state for which the known angular momentum and parity preclude any other l assignment. In Cd^{114} there is some question about interpreting the 1.906- and 1.976-MeV peaks as doublets, one member of which is excited by an $l=4$ transition, but other interpretations of the angular distributions would be difficult, and in any case, even if these peaks were assumed not to have $l=4$ components, the disagreement with Sn^{116} would still be substantial. In the Pd isotopes the $l=4$ assignments seem reasonably certain. Thus the best potential experimental explanations for the excessive $g_{7/2}$ strength and the deficiency in $h_{11/2}$ strength in (d,p) reactions in this region seem not to be applicable. This matter is now being further investigated with (d,t) pickup reactions, but it is already by far the most serious discrepancy with nuclear theory found in any of the long series of high-energy-resolution studies of stripping reactions at this laboratory.

In general, the agreements for the $s_{1/2}$, $d_{3/2}$, and $d_{5/2}$ states in Table III are about as good as can be expected. The large value of U_j^2 for $d_{3/2}$ in Cd^{114} is somewhat disturbing, but a rather large value was also found in the new measurements for $Sn^{116}(d,p)$, so this is perhaps due to an aberration in the DWBA at 12 MeV such as might be cured by a change in optical-model parameters.

The general agreement among E_j values in Table II is also reasonable, although there may be some significance in the fact that the $d_{3/2}$ single-quasiparticle state in Cd^{115} lies well above the $h_{11/2}$, whereas the reverse is true in Sn^{117}, and they are at nearly the same energy in In^{116}. There is no indication from the $g_{7/2}$ single-quasiparticle energy that that state is about half full as indicated in Table III. Single-quasiparticle energies are, however, quite sensitive to other interactions than the pairing force, so no great weight should be placed on this result.

ACKNOWLEDGMENT

The authors are greatly indebted to T. M. O'Keefe for permission to use some of his results from $Sn^{116}(d,p)$ prior to publication.